

## Effect of AC and Cu<sub>2</sub>O from Cu/Cu<sub>2</sub>O-AC/TiO<sub>2</sub> Composite Catalysts on the Photocatalytic Degradation of MO Under Visible Light

Ze-Da Meng, Trisha Ghosh, Jung-Hwan Cho, Lei Zhu, Chong-Yeon Park, Jong-Geun Choi, and Won-Chun Oh<sup>†</sup>

*Department of Advanced Materials Science & Engineering, Hanseo University, Seosan 356-706, Korea*

(Received September 10, 2011; Revised October 21, 2011; Accepted October 22, 2011)

### ABSTRACT

Activity carbon (AC), Cu and Cu<sub>2</sub>O modified TiO<sub>2</sub> composites (Cu/Cu<sub>2</sub>O-AC/TiO<sub>2</sub>) were prepared using a sol-gel method. The characteristics of the composites were evaluated using Brunauer-Emmett-Teller (BET) surface area measurements, X-ray diffraction (XRD), energy dispersive X-ray (EDX) analysis and scanning electron microscope (SEM) analysis. A methyl orange (MO) solution under visible light irradiation was used to determine the photocatalytic activity. The degradation of MO was determined using UV/Vis spectrophotometry. Cu<sub>2</sub>O, Cu and the cooperative effect of the AC increased the photo-absorption effect, thus increasing in photocatalytic activity.

**Key words:** Cu<sub>2</sub>O, AC, MO, Visible light, Photocatalytic

### 1. Introduction

Industrial dyestuffs, including textile dyes, are recognized as important environmental threats. Physical, chemical, and biological methods are available for the treatment of these wastes. The photocatalytic treatment using a TiO<sub>2</sub> photocatalyst shows promise for water purification, as many hazardous organic compounds can be decomposed and mineralized by the proceeding oxidation and reduction processes on the TiO<sub>2</sub> surface.<sup>1)</sup> Among the available photocatalysts, TiO<sub>2</sub> (in an anatase phase) has been most widely used because it is easily available, inexpensive, non-toxic, and shows relatively a high chemical stability.<sup>2-5)</sup>

However, the primary problem using TiO<sub>2</sub> photocatalysts is that they are only active under UV light irradiation with wavelengths shorter than 390 nm; thus only a small fraction (3-5%) solar irradiation can be used to degrade these environmental pollutants because of their wide band gap. To widen the area of their practical application under indoor use, photocatalysts active under visible light and giving a high yield are required. TiO<sub>2</sub>, having an energy band gap of about 3.2 eV, primarily absorbs the ultraviolet portion of the solar spectrum and only a small amount of visible light.<sup>6-8)</sup> Thus, for efficient photocatalytic activity, it is necessary to extend the photoresponsivity of TiO<sub>2</sub> to include the visible spectrum through the modification of its optical properties. Another problem is the high recombination rate of photo-generated electron-hole pairs that can be limited by introducing charge

traps for electrons and/or holes, thus prolonging the recombination time.<sup>9)</sup> Many methods have been proposed to solve these problems, but doping TiO<sub>2</sub> with foreign ions is one of the most promising strategies for sensitizing TiO<sub>2</sub> to visible light and also for forming charge traps to keep electron-hole pairs separated.<sup>10)</sup>

In 1998, Hara et al.<sup>11)</sup> discovered that Cu<sub>2</sub>O powder could catalyze the decomposition of water into H<sub>2</sub> and O<sub>2</sub> under solar light, in which Cu<sub>2</sub>O exhibited good catalytic performance and stability. Since the band gap potential of Cu<sub>2</sub>O is only 2.0 eV, electrons at the band gap are easily excited under visible light irradiation. However, it has the disadvantage of permitting the easy recombination of electron and hole results under the low catalytic activity of Cu<sub>2</sub>O.<sup>12)</sup> In order to control the rate of recombination, the composites of semiconductor materials possessing different band gaps were prepared and found to be able to suppress the electron-hole recombination, resulting in the better catalytic performance. Pure Cu has excited electrical conductivity, can act as transmitter, and enhance the photogeneration electrical transfer effect, thus increasing the photocatalytic activity.<sup>13)</sup>

Activity carbon (AC) is an excellent alternative because it can concentrate pollutants through adsorption around loaded TiO<sub>2</sub>, leading to an increase in the degradation of pollutants.<sup>14)</sup> Additionally, the interaction between the pollutants and the surface of the AC-TiO<sub>2</sub> was enhanced to promote further degradation.<sup>15)</sup> Consequently, the TiO<sub>2</sub>/AC is a promising photocatalyst with the prospective potential for industrial applications.<sup>16-19)</sup>

Until now, the sol-gel method has been used to produce TiO<sub>2</sub> nanostructures. In this work, the use of the sol-gel method was used to produce Cu/Cu<sub>2</sub>O-AC/TiO<sub>2</sub> compounds, and a different oxidizer was used to produce oxidized activity carbon.

<sup>†</sup>Corresponding author : Oh Won-Chun  
E-mail : wc\_oh@hanseo.ac.kr  
Tel : +82-41-660-1337 Fax : +82-41-688-3352

Alternatively oxidized carbon was used to produce Cu/Cu<sub>2</sub>O-AC/TiO<sub>2</sub> compounds, and their photocatalytic activity was compared under visible light.

## 2. Experimental Procedure

### 2.1. Materials

All chemicals were used as received without further purification. To obtain active carbon, a coconut-based precursor char purchased from Hanil Green Tec was used (Korea). The coconut shell was pre-carbonized first at 773 K, and then activated by steam diluted with nitrogen in a cylindrical quartz tube at 1023 K for 30 minutes. This AC was washed with deionized water and dried overnight in a vacuum drier at over 683 K.

MCPBA (*m*-Chloroperbenzoic acid) was purchased from New Jersey, USA. H<sub>2</sub>SO<sub>4</sub> and HNO<sub>3</sub> were purchased from Daejung Chemicals and Metals CO., LTD, Korea. CuSO<sub>4</sub>·5H<sub>2</sub>O was purchased from Duksan Pure Chemical CO., LTD, Korea. The titanium (IV) *n*-butoxide (TNB, C<sub>16</sub>H<sub>36</sub>O<sub>4</sub>Ti) used as the titanium source for the preparation of the Cu/Cu<sub>2</sub>O-AC/TiO<sub>2</sub> composites was reagent-grade and purchased from Acros Organics (USA). The Methyl Orange (MO, C<sub>14</sub>H<sub>14</sub>N<sub>3</sub>NaO<sub>3</sub>S, 99.9%, Duksan Pure Chemical Co., Ltd) was of analytical grade.

### 2.2. Chemical Oxidation on the AC Surface and Metal Treatment

These ACs were washed with deionized water and dried for 24 h at ambient temperature. The ACs were pulverized via a pulverizer. 20 g of carbon fiber materials was ball milled for 48 h at room temperature in a laboratory tumbling ball mill, and then the mechano-chemical carbon materials were obtained using a laboratory Pulverisette 6 mono-planetary high energy mill (Idar-Oberstein, Frisch, Germany) for 1 h with ZrO<sub>2</sub> balls (1 mm × 300 g).

#### 2.2.1. Oxidization Using H<sub>2</sub>SO<sub>4</sub> and HNO<sub>3</sub> Mixed Solution

A mixed solution of H<sub>2</sub>SO<sub>4</sub> and HNO<sub>3</sub> (volume ratio of 70 : 30, solution A) was used to oxidize the AC particles. 3 g of pulverized ACs were mixed within the 100 ml of solution A, stirred for 7-8 h and flushed with distilled water three times and dried at 323 K. Oxidized AC was formed (AC1).

#### 2.2.2. Oxidized by MCPBA

MCPBA (*m*-chloroperbenzoic acid, ca. 0.69 g) was suspended in 60 ml of benzene, followed by the addition of AC (ca. 2.5 g). MCPBA is used to oxidize the AC. The mixture was heated under reflux in air and stirred for 6h. The solvent was then dried at boiling point of benzene (353.13 K). After completion, the dark brown precipitates were washed with ethyl alcohol and dried at 323 K, resulting in the formation of oxidized AC (AC2).

#### 2.2.3. Oxidized by (NH<sub>4</sub>)<sub>2</sub>S<sub>2</sub>O<sub>8</sub>

(NH<sub>4</sub>)<sub>2</sub>S<sub>2</sub>O<sub>8</sub> was suspended in 100 ml H<sub>2</sub>O, followed by the addition of AC (ca. 3.0 g). The mixture was heated under

reflux in air and stirred for 6 h. The solvent was then dried at 353 K. After completion, the dark brown precipitates were washed with ethyl alcohol and water, dried at 323 K, resulting in the formation of oxidized AC (AC3).

#### 2.2.4. Metal Treatment

0.1 M CuSO<sub>4</sub>·5H<sub>2</sub>O solution was mixed with different oxidized AC, respectively. The resulting mixture was heated under reflux in air and stirred for 5 h at 343 K using a magnetic stirrer in a vial. After heat treatment at 873 K for 3 h, the Cu/Cu<sub>2</sub>O-AC composite was formed.

### 2.3. Preparation of Cu/Cu<sub>2</sub>O-AC/TiO<sub>2</sub> Composites

After washing the Cu/Cu<sub>2</sub>O-AC with ethanol several times, the Cu/Cu<sub>2</sub>O-ACs were prepared using pristine concentrations of TNB for the preparation of the Cu/Cu<sub>2</sub>O-AC/TiO<sub>2</sub> composites. Cu/Cu<sub>2</sub>O-AC powder was then mixed with 2 ml TNB. The solutions were then homogenized under reflux at 343 K for 3 h, while being stirred again in a vial. After stirring, the solution was transformed into Cu/Cu<sub>2</sub>O-AC/TiO<sub>2</sub> gels, which were heat treated at 773 K to produce the Cu/Cu<sub>2</sub>O-AC/TiO<sub>2</sub> composites.

### 2.4. Characterization of the Cu/Cu<sub>2</sub>O-AC/TiO<sub>2</sub> Compounds

XRD (Shimadzu XD-D1, Japan) with Cu K $\alpha$  radiation was used to examine the structural variations. The surface states and structures of the composites were examined by SEM (JSM-5200 JOEL, Japan). Energy dispersive X-ray (EDX) was also used for elemental analysis of the samples. The specific surface area (BET) was determined using N<sub>2</sub> adsorption measurements at 77 K (Monosorb, USA).

### 2.5. Photocatalytic Activities

A specified quantity of the photocatalyst composite was added to the 100 ml MO solution. The reactor was placed in the dark for 2 h to allow the maximum adsorption of MO molecules to the photocatalyst composite particles. In all experiments, the initial concentration of the MO was 1 × 10<sup>-5</sup> mol/L, and the amount of the photocatalyst composite was 0.01 g/ (100 ml solution). After adsorption, the photodecomposition of the MO solution was performed under visible light in a dark-box to ensure the reactor was irradiated by a single light source. The visible light source used was an LED lamp (18 W) with the main emission wavelength at 460 nm. The visible light irradiation of the photoreactor was performed for 30 min, 60 min, 90 min and 120 min. The experiments were performed at room temperature. In the process of MO degradation, a glass reactor was used and the reactor was placed on a magnetic churn dasher. Samples were then withdrawn regularly from the reactor and the dispersed powders were removed by a centrifuge. The MO concentration in the solution was then determined as a function of the irradiation time from the change in absorbance at a wavelength of 660 nm. After treatment with the centrifuge the centrifugalizations were analyzed using a UV-vis spectrophotometer.

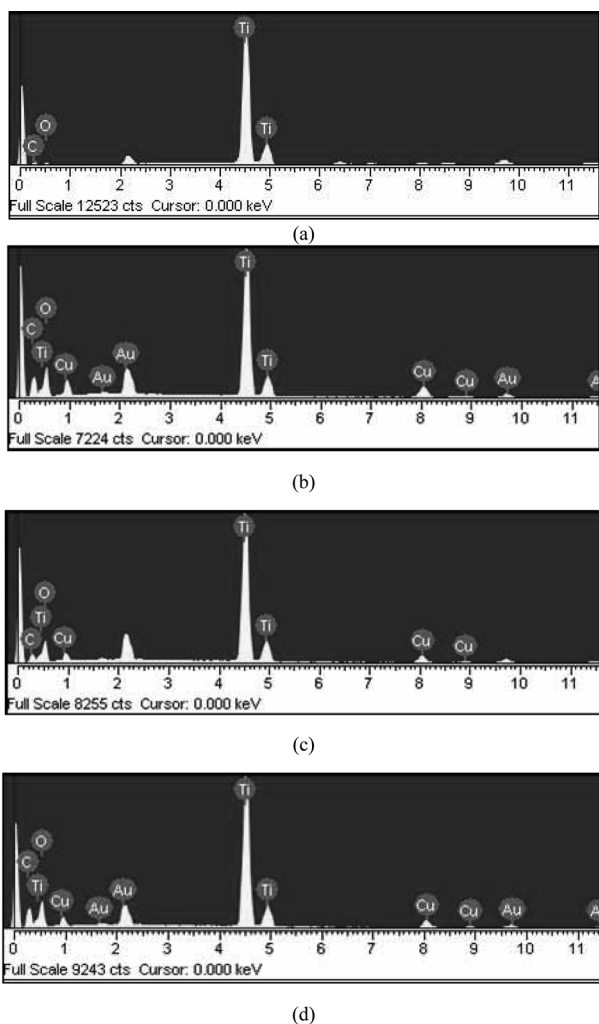


**Fig. 1.** EDX elemental microanalysis of photocatalysts, (a) AC-TiO<sub>2</sub>, (b) CuACT1, (c) CuACT2, and (d) CuACT3.

### 3. Results and Discussion

#### 3.1. Elemental Analysis of the Samples

Fig. 1 shows the EDX patterns of the AC-TiO<sub>2</sub>, CuACT1, CuACT2 and CuACT3. The elemental composition of these samples was analyzed and the characteristic elements were identified. Fig. 1 shows strong K $\alpha$  and K $\beta$  peaks from Ti at 4.51 and 4.92 keV, whereas a moderate K $\alpha$  peak for O appears at 0.52 keV.<sup>20</sup> In addition to the above peaks, Cu was also observed. Fig. 1 presents the quantitative microanalysis of C, O, Ti and Cu as the major elements for the composites by EDX. Table 1 lists the composition ratios of the samples. There were some small impurities, which are believed to have been introduced from the unpurified AC or CuSO<sub>4</sub>·5H<sub>2</sub>O. In the case of most samples, tungsten, carbon and titanium were present as major elements with small quantities of oxygen in the composite (shown in Table 2).

#### 3.2. Surface Characteristics of the Samples

Fig. 2 shows the SEM images of the micro-surface structures

**Table 1.** Nomenclature of Samples Prepared with Photocatalysts

Preparation method	Nomenclatures
3 g AC + MCPBA + 2 ml TNB	AC-TiO <sub>2</sub>
3 g AC + H <sub>2</sub> SO <sub>4</sub> /H <sub>2</sub> NO <sub>3</sub> (AC1) + 2 ml TNB + 0.1 m CuSO <sub>4</sub> ·5H <sub>2</sub> O	CuACT1
2.5 g AC + MCPBA (AC2) + 2 ml TNB + 0.1 m CuSO <sub>4</sub> ·5H <sub>2</sub> O	CuACT2
3 g AC + (NH <sub>4</sub> ) <sub>2</sub> S <sub>2</sub> O <sub>4</sub> (AC3) + 2 ml TNB + 0.1 m CuSO <sub>4</sub> ·5H <sub>2</sub> O	CuACT3

**Table 2.** EDX Elemental Microanalysis and BET Surface Area

Sample name	C (%)	O (%)	Cu (%)	Impurity (%)	Ti (%)	BET (m <sup>2</sup> /g)
TiO <sub>2</sub>	–	–	–	0.01	99.99	18.95
AC-TiO <sub>2</sub>	20.72	44.11	–	1.12	34.05	136.25
CuACT1	17.96	30.34	21.66	0.15	21.59	32.20
CuACT2	20.47	36.24	17.21	0.14	25.88	51.24
CuACT3	30.21	26.52	17.18	0.40	25.68	47.26

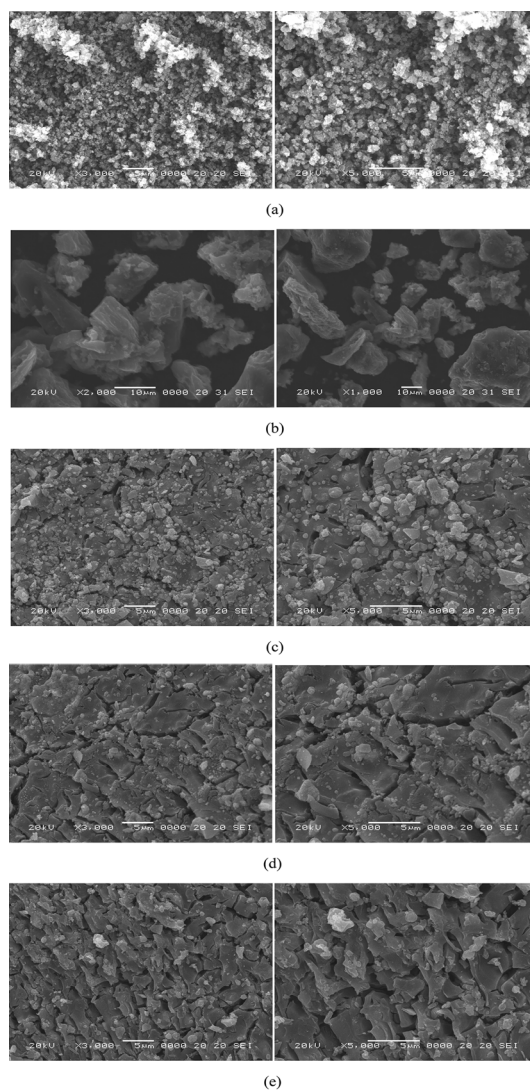


**Fig. 2.** SEM images of (a) pure TiO<sub>2</sub>, (b) AC-TiO<sub>2</sub>, (c) CuACT1, (d) CuACT2, and (e) CuACT3.

and the morphology of the compounds. The  $\text{TiO}_2$  and metal particles uniformly coated the AC surface, which led to an increase in nanoparticle size. Zhang *et al.* reported that a good dispersion of small particles could provide more reactive sites for the reactants than aggregated particles.<sup>21)</sup> The surface roughness appears high due to some grain aggregation. Fig. 2(a) shows the SEM images of the pure  $\text{TiO}_2$ , and the pure  $\text{TiO}_2$  has a good dispersion of small particles. Fig. 2(b) shows the SEM images of AC- $\text{TiO}_2$ . It is possible to locate the AC particles from the SEM image. Figs. 2(c), (d) and (e) show the SEM images of CuACT1, CuACT2 and CuACT3, respectively. From the SEM image we can see the  $\text{TiO}_2$  and metal particles uniformly coated the AC surface. Comparing Figs. 2(a), (b) and (c), we can determine that the level of aggregation increased. Figs. 2(c), (d) and (e) show that the CuACT3 has a good dispersion and relatively smaller particles. When the AC was oxidized by  $(\text{NH}_4)_2\text{S}_2\text{O}_8$  the function groups showed good dispersion. The function groups were coupled with copper, cuprous oxide and  $\text{TiO}_2$ . The function groups had good dispersion on the surface of the AC, which causes a good dispersion state in the compounds and causes smaller particles.<sup>22,23)</sup>

Table 2 lists the BET surface areas of the samples. The BET surface areas of pristine  $\text{TiO}_2$ , as well as the prepared AC- $\text{TiO}_2$ , CuACT1, CuACT2 and CuACT3 were  $136.25 \text{ m}^2/\text{g}$ ,  $32.20 \text{ m}^2/\text{g}$ ,  $51.24 \text{ m}^2/\text{g}$  and  $47.26 \text{ m}^2/\text{g}$ , respectively. The  $\text{TiO}_2$  and copper particles were introduced to the pores of the AC, which decreased the BET surface area. The AC- $\text{TiO}_2$  sample had the largest area, which can affect the adsorption reaction. The BET surface area of the photocatalyst CuACT decreased when ACF/ $\text{WO}_3$  particles were doped with copper. This is because copper particles fill the pores of the AC- $\text{TiO}_2$  particles,<sup>24)</sup> thereby reducing the pore size and pore volume of the AC- $\text{TiO}_2$  particles (showed in Table 2).

### 3.3. Structural Analysis

Fig. 3 shows the XRD patterns of the pure  $\text{TiO}_2$ , AC- $\text{TiO}_2$ , CuACT1, CuACT2 and CuACT3 composites. After heat

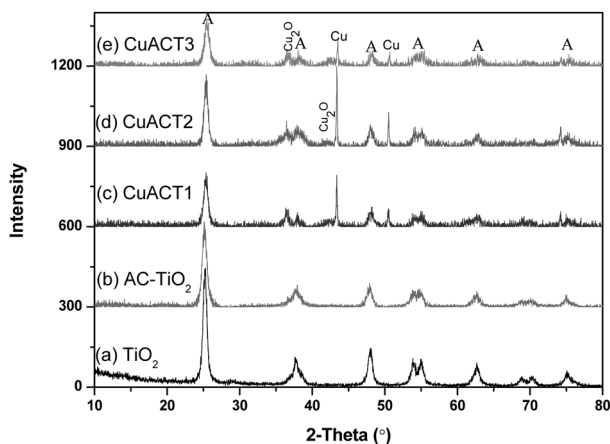


Fig. 3. The XRD patterns of (a) pure  $\text{TiO}_2$ , (b) AC- $\text{TiO}_2$ , (c) CuACT1, (d) CuACT2, and (e) CuACT3.

treatment at 773 K, major peaks were observed at  $25.3^\circ$ ,  $37.9^\circ$ ,  $48.0^\circ$ ,  $53.8^\circ$ ,  $54.9^\circ$ , and  $62.5^\circ$  (2 $\theta$ ), which were assigned to the (101), (004), (200), (105), (211), and (204) planes of anatase, indicating that the prepared  $\text{TiO}_2$  is anatase.<sup>25)</sup> These results suggest that AC- $\text{TiO}_2$  and CuACT also has a pure anatase phase structure under the current preparation conditions. The XRD pattern shows peaks characteristics of  $\text{Cu}_2\text{O}$  and Cu. Additional  $\text{Cu}_2\text{O}$  diffraction peaks for the (111) and (200) planes were observed at  $36.46^\circ$  and  $42.32^\circ$  (2 $\theta$ ), respectively.<sup>26)</sup> All the diffraction characteristic peaks of the  $\text{Cu}_2\text{O}$  species in XRD can be readily assigned to the crystalline phase  $\text{Cu}_2\text{O}$  in a cubic structure. The peaks of Cu were observed in the XRD pattern of the CuACT compound for the (111) and (200) planes at  $43.33^\circ$  and  $50.64^\circ$  (2 $\theta$ ). However, the peak intensity of  $\text{Cu}_2\text{O}$  and Cu were fairly weak. In the AC- $\text{TiO}_2$  and CuACT composite's XRD pattern, the intensity of the peaks concerning  $\text{TiO}_2$  was decreased. This is because the  $\text{TiO}_2$  content in the samples was decreased and this in turn influenced the  $\text{Cu}_2\text{O}$  and Cu peaks. It is believed that some other peaks were introduced from the unpurified  $\text{CuSO}_4 \cdot 5\text{H}_2\text{O}$  hydrate and TNB.

### 3.4. Photocatalytic Activity of Samples

Fig. 4 shows the time series of MO degradation using pure  $\text{TiO}_2$ , AC- $\text{TiO}_2$ , and CuACT1 under visible light irradiation. The spectra for the MO solution after visible light irradiation show the relative degradation yields at different irradiation times. The decreases in dye concentration continued with an oppositely gentle slope, which was due to the visible light irradiation. The concentration of MO was  $1.0 \times 10^{-5} \text{ mol/L}$ , and the absorbance for MO decreased as the irradiation time under visible increased. Moreover, the MO solution increasingly lost its color, and the MO concentration continued to decrease. Two steps are involved in the photocatalytic decomposition of dyes; the adsorption of dye molecules and degradation. After adsorption in the dark for 2 h, the samples reached adsorption-desorption equilibrium. In the adsorptive step, pure  $\text{TiO}_2$ , AC- $\text{TiO}_2$ , and CuACT1 composites showed different

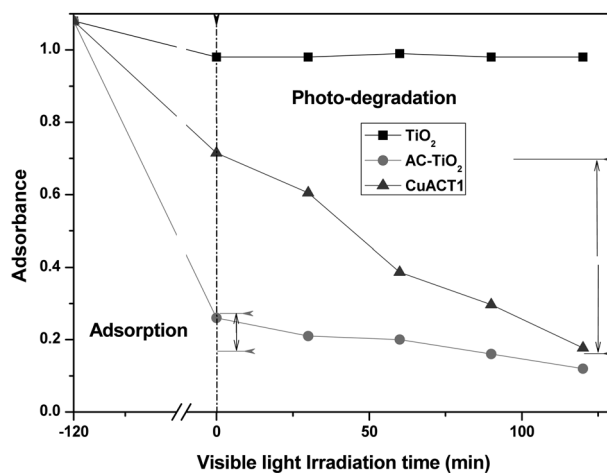


Fig. 4. Decolorization effect on MO of pure  $\text{TiO}_2$ , AC- $\text{TiO}_2$  and CuACT1.

adsorptive effects with AC-TiO<sub>2</sub> having the best adsorptive effect. The adsorptive effect of pure TiO<sub>2</sub> was the lowest. AC-TiO<sub>2</sub> has the largest BET surface area, which can enhance the adsorptive effect. In the degradation step, the CuACT1 composites showed a good degradation effect. A comparison of the decolorization effect of the catalysts showed that CuACT1 composites had the best degradation effect, which is due to the synergistic reaction of Cu<sub>2</sub>O, Cu, AC and TiO<sub>2</sub>.

Fig. 5 shows the time series of MO degradation using CuACT1, CuACT2 and CuACT3 composites. In the adsorptive step, CuACT1, CuACT2 and CuACT3 composites showed different adsorptive effects with AC-TiO<sub>2</sub> having the best adsorptive effect. The adsorptive effect of pure TiO<sub>2</sub> was the lowest. AC-TiO<sub>2</sub> has the largest BET surface area, which can enhance the adsorptive effect. In the degradation step, the CuACT2 composites showed a good degradation effect.

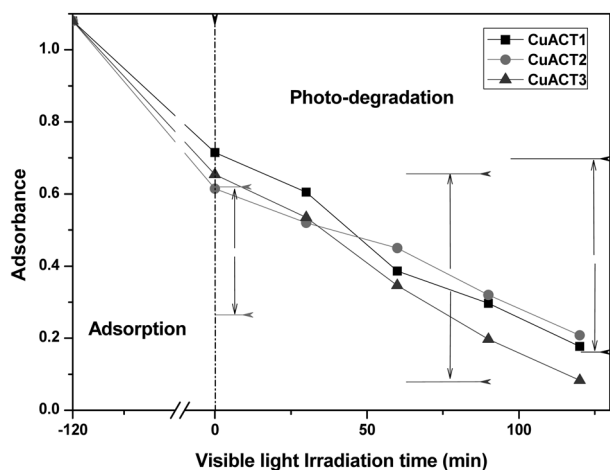


Fig. 5. Decolorization effect on MO of CuACT1, CuACT2 and CuACT3.

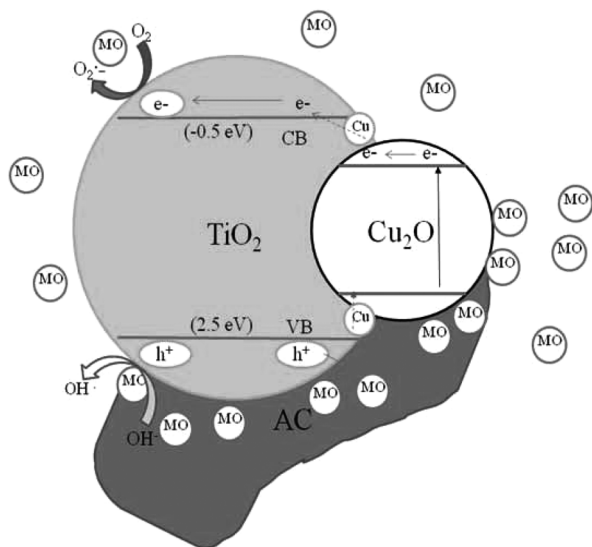


Fig. 6. Schematic diagram of the separation of photogenerated electrons and holes on the photocatalytic interface.

A comparison of the decoloration effect of the catalysts showed that CuACT3 composites have best degradation effect.

Fig. 6 is the schematic diagram of the separation of the photogenerated electrons and holes on the photocatalytic interface. Both the minimum conduction band and the maximum valence band of Cu<sub>2</sub>O lie above those of TiO<sub>2</sub>; therefore the electrons excited to the conduction band of the Cu<sub>2</sub>O would transfer to the TiO<sub>2</sub>, whereas the holes generated in the valence band in the TiO<sub>2</sub> prefer an opposing transfer to the Cu<sub>2</sub>O. Charge carriers separated in different semiconductors effectively reduce the chance of electron-hole pair recombination and prolong their lifetime, thus increasing their quantum efficiencies. In addition, the working range of the wavelength is extended to a visible region due to absorption of visible light by Cu<sub>2</sub>O, further enhancing the efficiency of the solar energy transition. Synergistic cooperation of these effects enables the Cu<sub>2</sub>O/TiO<sub>2</sub> system to exhibit great potential for solar cell and photocatalysis applications.<sup>27-30</sup> AC acts as the adsorb effect, and increases the surface area of the compounds which can increase the adsorption effect for samples, adsorbing more O<sub>2</sub> and dye molecules, and ensuring these systems take full advantage of yield oxidizing species. The Cu has excited electrical conductivity, and can act as a transmitter, and enhance the photogenerate electrical transfer effect, thus increasing the photocatalytic activity. The positive holes in the valence band can be trapped by OH or H<sub>2</sub>O species adsorbed on the surface of the catalyst, producing reactive hydroxyl radicals in aqueous media. The photo-generated electrons accumulate on the surface of TiO<sub>2</sub> and could be rapidly transferred to molecular oxygen O<sub>2</sub> to form the superoxide radical anion O<sub>2</sub><sup>-</sup> and hydrogen peroxide H<sub>2</sub>O<sub>2</sub>. The oxidative degradation of dyes was caused by the attack of hydroxyl radicals and superoxide ions, which are the highly reactive electrophilic oxidants. Due to the efficiency of hydroxyl radicals and superoxide ions, azo dyes decomposed to CO<sub>2</sub>, H<sub>2</sub>O and small inorganic molecules.<sup>31</sup>

#### 4. Conclusions

This study examined the preparation and characterization of AC-TiO<sub>2</sub> and CuACT compounds. The BET surface area of AC-TiO<sub>2</sub> was higher than that of the CuACT composite. The SEM image shows that CuACT3 has a good dispersion and relatively smaller particles. XRD revealed the crystal structure of Cu and the cubic structure of the Cu<sub>2</sub>O. The CuACT had a good photo-degradation effect under visible light irradiation, due to the photosensitivity of Cu<sub>2</sub>O, and enhanced the BET surface area effect of the ACF. The CuACT3 composite showed the best photocatalytic degradation activity of the MO solutions under visible light irradiation. This was attributed to the three different effects between the photocatalytic reaction of the supported TiO<sub>2</sub>, the energy transfer effects of Cu<sub>2</sub>O and Cu, such as electrons and light, and the separation effect in this system.

#### REFERENCES

1. E. Piera, M. I. Tejedor, M. E. Zorn, and M. A. Anderson,

- "Degradation of Chlorophenols by Means of Advanced Oxidation Processes: a General Review," *Appl. Catal. B: Environ.*, **47** 219-56 (2004).
2. A. Fujishima, K. Hashimoto, and T. Watanabe, "TiO<sub>2</sub> Photocatalysis Fundamentals and Applications," *BKC. Inc.*, May (1999).
  3. W. C. Oh, "Review of Carbon Based Titania Photocatalysts," *J. Photo. Sci.*, **1** 29-34 (2010).
  4. Z. D. Meng and Oh W. C. Oh, "Photocatalytic Degradation of Methylene Blue on Fe-fullerene/TiO<sub>2</sub> Under Visible-light Irradiation," *Asian J. Chem.*, **23** 847-52 (2011).
  5. W. C. Oh and F. J. Zhang, "A Review of Antibacterial Activity of CNT/TiO<sub>2</sub>, Ag- CNT/TiO<sub>2</sub>, and C<sub>60</sub>/TiO<sub>2</sub>," *J. Photo. Sci.*, **1** 63-7 (2010).
  6. C. G. Silva, W. Wang, and J. L. Faria, "Photocatalytic and Photochemical Degradation of Mono-, Di- and Tri-azo Dyes in Aqueous Solution under UV Irradiation," *J. Photochem. Photobiol. A: Chem.*, **181** 314-24 (2006).
  7. V. Shah, P. Verma, P. Stopka, J. Gabriel, P. Baldrian, and F. Nerud, "Decolorization of Dyes with Copper (II)/organic acid/hydrogen Peroxide Systems," *Appl. Catal. B: Environ.*, **46** 287-92 (2003).
  8. I. K. Konstantinou and T. A. Albanis, "Photocatalytic Transformation of Pesticides in Aqueous Titanium Dioxide Suspensions using Artificial and Solar Light: Intermediates and Degradation Pathways," *Appl. Catal. B: Environ.*, **42** 319-35 (2003).
  9. T. Sauer, G. Cesconeto Neto, H. J. Jose, and R. F. P. M. Moreira, "Kinetics of Photocatalytic Degradation of Reactive Dyes in a TiO<sub>2</sub> Slurry Reactor," *J. Photochem. Photobiol. A: Chem.*, **149** 147-54 (2002).
  10. Z. D. Meng, K. Zhang, and W. C. Oh, "Preparation of Different Fe Containing TiO<sub>2</sub> Photocatalysts and Comparison of Their Photocatalytic Activity," *Kor. J. Mater. Res.*, **20** 228-34 (2010).
  11. M. Hara, T. Kondo, M. Komoda, S. Ikeda, K. Shinohara, A. Tanaka, J. N. Kondo, and K. Domen, "Cu<sub>2</sub>O as a Photocatalyst for Overall Water Splitting under Visible Light Irradiation," *Chem. Commun.*, **3** 357-58 (1998).
  12. M. K. I. Senevirathna, P. K. D. D. P. Pitigala, and K. Tenakone, "Water Photoreduction with Cu<sub>2</sub>O Quantum Dots on TiO<sub>2</sub> Nano-particles," *J. Photochem. Photobiol. A: Chem.*, **171** 257-59 (2005).
  13. Y. Bessekhoud, D. Robert, and J. V. Weber, "Photocatalytic Activity of Cu<sub>2</sub>O/TiO<sub>2</sub>, Bi<sub>2</sub>O<sub>3</sub>/TiO<sub>2</sub> and ZnMn<sub>2</sub>O<sub>4</sub>/TiO<sub>2</sub> Heterojunctions," *Catal. Today*, **101** 315-21 (2005).
  14. T. Torimoto, S. Ito, S. Kuwabata, and H. Yoneyama, "Effects of Adsorbents used as Supports for Titanium Dioxide Loading on Photocatalytic Degradation of Propylamide," *Environ. Sci. Technol.*, **30** 1275-281 (1996).
  15. J. Araña, J. M. Doña-Rodríguez, E. Tello Rendón, C. Garriga i Cabo, O. González-Díaz, J. A. Herrera-Melián, J. Pérez-Peña, G. Colón and J. A. Navío, "TiO<sub>2</sub> Activation by using Activated Carbon as a Support. Part II. Photoreactivity and FTIR study," *Appl. Catal. B: Environ.*, **44** 153-60 (2003).
  16. X. W. Zhang and L. C. Lei, "Effect of Preparation Methods on the Structure and Catalytic Performance of TiO<sub>2</sub>/AC Photocatalysts," *J. Hazardous Mater.*, **153** 827-33 (2008).
  17. Z. D. Meng, M. L. Chen, F. J. Zhang, L. Zhu, J. G. Cho, and W. C. Oh, "Rare Earth Oxide Doped Fullerene and Titania Composites and Photocatalytic Properties of Methylene Blue Under Visible Light," *Asian J. Chem.*, **23** 2327-331 (2011).
  18. W. C. Oh, J. H. Son, F. J. Zhang, and M. L. Cheng, "Fabrication of Ni-AC/TiO<sub>2</sub> Composites and Their Photocatalytic Activity for Degradation of Methylene Blue," *J. Kor. Ceram. Soc.*, **46** [1] 1-9 (2009).
  19. W. C. Oh, A. R. Jung, and W. B. Ko, "Characterization and Relative Photonic Efficiencies of a New Nanocarbon/TiO<sub>2</sub> Composite Photocatalyst Designed for Organic Dye Decomposition and Bactericidal Activity," *Mater. Sci. Eng. C*, **29** 1338-47 (2009).
  20. Z. D. Meng and W. C. Oh, "Sonocatalytic Degradation and Catalytic Activities for MB Solution of Fe Treated Fullerene/TiO<sub>2</sub> Composite with Different Ultrasonic Intensity," *Ultras. Sonochem.*, **18** 757-61 (2011).
  21. X. W. Zhang, M. H. Zhou, and L. C. Lei, "Preparation of Photocatalytic TiO<sub>2</sub> Coating of Nanosized Particles Supported on Activated Carbon by AP-MOCVD," *Carbon*, **43** 1700-708 (2005).
  22. H. Hidaka, H. Kubota, M. Gratzel, E. Pelizzetti, and N. Serpone, "Photodegradation of Surfactants. II. Degradation of Sodium Dodecylbenzene Sulphonate Catalysed by Titanium Dioxide Particles," *J. Photochem.*, **35** 219-30 (1986).
  23. A. M. Amat, A. Arques, M. A. Miranda, and S. Seguí, "Photo-Fenton Reaction for the Abatement of Commercial Surfactants in a Solar Pilot Plant," *Solar Energy*, **77** 559-66 (2004).
  24. Z. D. Meng, L. Zhu, J. G. Choi, F. J. Zhang, and W. C. Oh, "Effect of Pt Treated Fullerene/TiO<sub>2</sub> on the Photocatalytic Degradation of MO Under Visible Light," *J. Mater. Chem.*, **21** 7596 (2011).
  25. J. Bandara, C. P. K. Udawatta, and C. S. K. Rajapakse, "Highly Stable CuO Incorporated TiO<sub>2</sub> Catalyst for Photocatalytic Hydrogen Production from H<sub>2</sub>O," *Photochem. Photobiol. Sci.*, **4** 857-61 (2005).
  26. J. L. Li, L. Liu, Y. Yu, Y. W. Tang, H. L. Li, and F. P. Du, "Preparation of Highly Photocatalytic Active Nano-size TiO<sub>2</sub>-Cu<sub>2</sub>O Particle Composites with a Novel Electrochemical Method," *Electrochem. Commun.*, **6** 940-43 (2004).
  27. C. H. Han, Z. Y. Li, and J. Y. Shen, "Photocatalytic Degradation of Dodecyl-benzenesulfonate Over TiO<sub>2</sub>-Cu<sub>2</sub>O Under Visible Irradiation," *J. Hazardous Mater.*, **168** 215-19 (2009).
  28. F. R. Xiu and F. S. Zhang, "Preparation of nano-Cu<sub>2</sub>O/TiO<sub>2</sub> Photocatalyst from Waste Printed Circuit Boards by Electrokinetic Process," *J. Hazardous Mater.*, **172** 1458-63 (2009).
  29. X. D. Su, J. Z. Zhao, Y. L. Li, Y. C. Zhu, X. K. Ma, F. Sun, and Z. C. Wang, "Solution Synthesis of Cu<sub>2</sub>O/TiO<sub>2</sub> Core-shell Nanocomposites," *Colloids Surf, A: Physicochem. Eng. Aspects*, **349** 151-55 (2009).
  30. Y. Zhang, L. Ma, J. Li, and Y. Yu, "In situ Fenton Reagent Generated from TiO<sub>2</sub>/Cu<sub>2</sub>O Composite Film: A New way to Utilize TiO<sub>2</sub> Under Visible Light Irradiation," *Environ. Sci. Technol.*, **41** 6264-269 (2007).
  31. Z. D. Meng, L. Zhu, J. G. Choi, C. Y. Park, and W. C. Oh, "Preparation, Characterization and Photocatalytic Behavior of WO<sub>3</sub>-fullerene/TiO<sub>2</sub> Catalysts Under Visible Light," *Nanoscale Res. Lett.*, **6** 459 (2011).